Resonantly Tunable Majorana Polariton in a Microwave Cavity

Mircea Trif and Yaroslav Tserkovnyak

Department of Physics and Astronomy, University of California, Los Angeles, California 90095, USA

(Received 13 February 2012; published 21 December 2012)

We study the spectrum of a one-dimensional Kitaev chain placed in a microwave cavity. In the off-resonant regime, the frequency shift of the cavity can be used to identify the topological phase transition of the coupled system. In the resonant regime, the topology of the system is sensitive to the presence of photons in the microwave cavity and, moreover, for a large number of photons (classical limit), the physics becomes similar to that of periodically driven systems (Floquet insulators). We also analyze numerically a finite chain and show the existence of a degenerate subspace in the presence of the cavity that can be interpreted as a *Majorana polariton*.

DOI: 10.1103/PhysRevLett.109.257002 PACS numbers: 74.20.Mn, 03.67.Lx, 42.50.Pq, 74.81.Fa

Introduction.—Majorana fermions, or half-fermions, have recently attracted tremendous attention as building blocks of a topological quantum computer [1,2]. They are predicted to emerge as excitations in several solid-state systems, such as genuine two-dimensional (2D) p-wave superconductors [3], or induced via superconducting proximity effects in topological insulators [4–6] or one-dimensional (1D) wires [7] as boundary zero modes. They obey non-Abelian statistics, both in 2D [8] and 1D [9], allowing for implementation of certain (nonuniversal) gate operations required in quantum-computational schemes via braiding of the Majorana fermions. Moreover, due to their highly nonlocal character, the qubits built out of Majorana fermions are insensitive to local parity-conserving perturbations, thus making them potentially robust against physical noise errors [1,2,10,11].

The existence of Majorana states, however, has been shown not only for static systems, but also for driven systems, as zero modes in the so-called Floquet Hamiltonians [12], or even, more recently, in dissipative systems [13]. These proposals are based on the idea that driven systems can have different topology from their static parents, albeit these are not actual ground states. The ground-state perspective can, however, be used even for the driven models, if instead of a classical driving one considers the driving as having its own quantum dynamics, such as in a high-Q electromagnetic cavity. In particular, 1D microwave cavities have been proven extremely successful in reaching the so-called strong-coupling regime between photons and different types of qubits [14], with very large Q factors and a high degree of control. Moreover, strong coupling between atomic gases (e.g., in a Bose-Einstein condensate) and optical cavities has been achieved with a high degree of coherence [15]. In this Letter, we combine cavity QED with Majorana physics in a 1D lattice model. We analyze the spectrum of a p-wave lattice superconductor (Kitaev chain) coupled to a microwave cavity and examine the topology of the combined system. The spectrum is studied using a Dicke-like Hamiltonian, in both the off- and on-resonant regimes.

The model.—In Fig. 1, we show a schematic of the system under consideration: a Kitaev chain [1] inserted in a 1D microwave cavity. The physical sites are depicted by black ovals, while the constituent Majoranas are shown inside by solid red circles. The hopping parameter t and the chemical potential μ can be modified by the (quantum) cavity electric field $\hat{\boldsymbol{E}}(z)$, engendering a physical coupling between electrons and photons. The associated wavelength is assumed to be much larger than the 1D chain, so that the electric field has no spatial dependence along the latter.

The total Hamiltonian of the system, $\mathcal{H} = H_{\rm 1D} + H_{\rm int} + H_{\rm ph}$, consists of

$$H_{\rm 1D} = -\frac{1}{2}\sum_{j=1}^{N-1}(tc_{j+1}^{\dagger}c_j + \Delta c_{j+1}^{\dagger}c_j^{\dagger}) + \text{H.c.} - \mu\sum_{j=1}^{N} c_j^{\dagger}c_j,$$

$$H_{\rm int} = \left(\frac{\beta}{2}\sum_{j=1}^{N} c_{j+1}^{\dagger}c_j + \text{H.c.} + \alpha\sum_{j=1}^{N} c_j^{\dagger}c_j\right)(a^{\dagger} + a), \quad (1)$$

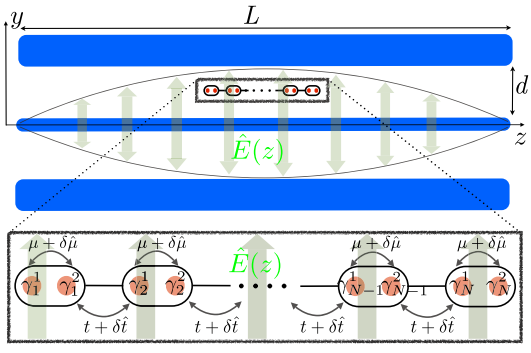

FIG. 1 (color online). A sketch of the system. In blue (light-gray) is the superconducting microwave cavity of length L, which supports quantized electromagnetic modes. The Majorana chain $\gamma_{1,2}^{1}\ldots\gamma_{N}^{1,2}$ is depicted inside the cavity with the relevant parameters renormalized due to the coupling to the cavity: Chemical potential $\mu \to \mu + \delta\hat{\mu}$ and hopping amplitude $t \to t + \delta\hat{t}$ (with the hats denoting fluctuating quantum contributions).

and $H_{\rm ph} = \omega a^\dagger a$, where t is the hopping parameter, Δ is the proximity-induced p-wave pairing potential [7], μ is the chemical potential, α is the electron-photon coupling that shifts the chemical potential, and β accounts for changes in the tunneling Hamiltonian linear in the photon field (which would be present in a wire with a structural asymmetry in the y direction; see Fig. 1). For simplicity we are assuming that the pairing potential Δ is unaffected by the photon field (see Supplemental Material [16], however). a ($a^\dagger$) stands for the photon creation (annihilation) operator and ω is the frequency of the corresponding photon mode (setting $\hbar = 1$ throughout). The electric field inside the cavity (corresponding to its fundamental harmonic) is $\hat{\boldsymbol{E}}(z) = \hat{\boldsymbol{e}}_y\sqrt{\omega/Ld^2c}\sin(\pi z/L)(a^\dagger + a)$ [14], with L being the cavity length, d is the distance between the center conductor and the ground conductors (see Fig. 1), and c is the capacitance per unit length. Note that the maximum of the electric field is at $z = L/2$, where the cavity-wire coupling is strongest. For the electrostatic interaction of the wire with the cavity mode [α term in Eq. (1)], we are supposing that the wire's Josephson coupling to a superconducting reservoir is strong enough that the phase of the proximity-induced Δ is anchored at a constant value corresponding to that of the reservoir. We note that either α or β coupling above would be sufficient for our purposes, but include both terms for completeness.

Isolated wire.—We begin by recapping some of the known results on the Majorana physics in 1D p-wave superconductors. To keep the ideas transparent (but without loss of generality), we assume in this section real $t = \Delta > 0$ and $\mu = 0$. Performing the substitutions $\gamma_j^1 = c_j^\dagger + c_j$ and $\gamma_j^2 = i(c_j - c_j^\dagger)$, in terms of Majorana operators, $(\gamma_j^i)^\dagger = \gamma_j^i$, with $i = 1, 2$, we can write the 1D wire Hamiltonian simply as $H_{\rm 1D} = -it\sum_{j=1}^{N-1}\gamma_j^2\gamma_{j+1}^1$, with γ_1^1 and γ_N^2 dropping out entirely. This guarantees a degenerate ground state, which can be viewed as a qubit indexed by $\sigma_z \equiv (c_F^\dagger c_F - 1/2)$. $c_F = (\gamma_1^1 + i\gamma_N^2)/2$ here is the *nonlocal* fermionic operator defining the corresponding zero-mode quasiparticle.

The existence of the Majorana end modes can be identified using bulk properties only, as they are a consequence of the topology of the Brillouin zone. Using periodic boundary conditions allows us to switch to the reciprocal space using $c_j = \sum_k c_k \exp(-ikj)/\sqrt{N}$ to write $\mathcal{H}_{\rm 1D} = \sum_{k>0} H_{\rm BdG}(k)$, where

$$H_{\rm BdG}(k) = -(t\cos k + \mu)\tau_k^z + t\sin k\tau_k^y \qquad (2)$$

is the Bogoliubov–de Gennes Hamiltonian (restoring a finite μ), and the pseudospin $\boldsymbol{\tau}_k = (\tau_k^x, \tau_k^y, \tau_k^z)$, expressed in terms of the Pauli matrices, acts on the particle-hole basis $(c_k, c_{-k}^\dagger)$. One can diagonalize this Hamiltonian $\tilde{H}_{\rm BdG}(k) = U^\dagger(k)H_{\rm BdG}(k)U(k)$ by $U(k) = \exp(-i\theta_k\tau_k^x/2)$, which gives $\tilde{H}_{\rm BdG} = -\epsilon_k\tau_k^z$, with $\epsilon_k = \sqrt{t^2 + \mu^2 + 2t\mu\cos k}$ and $\theta_k = \arctan[t\sin k/(t\cos k + \mu)]$. The topological invariant (winding number) that measures the number of edge modes at each end of the wire reads [17]:

$$P = \oint \frac{d\theta_k}{2\pi} \qquad (3)$$

and gives $P = 0$ (1) for $t < |\mu|$ ($t > |\mu|$), implying the absence (existence) of Majorana end modes for a system with open boundaries. We will now analyze this quantity in the presence of the cavity.

Cavity-coupled wire.—The combined system Hamiltonian can be mapped to the well-known Dicke model, namely a set of spins interacting with the same photonic mode. We start with the bulk system, later focusing on a finite wire. In the continuum limit, we can write the interaction Hamiltonian as $H_{\rm int} = \alpha\sum_k \delta_k(a^\dagger + a)\tau_k^z$, with $\delta_k = 1 + (\beta/\alpha)\cos k$, which resembles the interaction Hamiltonian between a photonic mode and a collection of spins: the Dicke model. To analyze the effect of this term on the spectrum, we consider both the high-frequency ($\omega \gg t + |\mu|$, i.e., much larger than the quasiparticle band width) and the resonant ($||t - |\mu|| < \omega < t + |\mu|$) regimes.

Off-resonant coupling.—For a large cavity detuning, $\omega \gg t + |\mu|$, all the transitions are off diagonal, and we can employ second-order perturbation theory using the Schrieffer-Wolff formalism. This means diagonalizing the Hamiltonian in a decoupled basis of the wire-cavity system via a unitary transformation, $\tilde{\mathcal{H}} = \exp(S)\mathcal{H}\exp(-S) = \mathcal{H} + [S, \mathcal{H}] + \mathcal{O}(S^2)$, with $S^\dagger = -S$ being an anti-Hermitian operator. We leave the details for the Supplemental Material [16] and only mention that, although in this situation the photon field cannot easily change the topology of the system, one can utilize the coupling to measure the topological phase of the system [18] as well as the transition point. This is encoded in the cavity frequency shift $\delta\omega = 2Nt(\alpha/\omega)^2\Gamma(\mu/t)$ with

$$\Gamma(\mu/t) \simeq \frac{2}{N}\sum_k \delta_k^2 \sin k\langle\tau_k^y\rangle \approx \frac{1}{2\pi}\int_0^\pi dk\,\delta_k^2\sin k\langle\tau_k^y\rangle, \qquad (4)$$

where $\langle\cdots\rangle$ means averaging over the (mean-field) ground state of the 1D system. The perturbative treatment is justified for finite-size chains with $\alpha\sqrt{N} \ll \omega$. Moreover, we note that besides the frequency shift, the cavity leads to a shift of the effective chemical potential, which is small in the perturbative regime (see the Supplemental Material [16]). In Fig. 2, we plot $\Gamma(x)$ and $\Gamma_2(x) \equiv d^2\Gamma/dx^2$ as a function of the chemical potential μ. We see that while $\Gamma(x)$ varies smoothly, $\Gamma_2(x)$ becomes singular at the topological transition point, the divergence being logarithmic in nature, i.e., $\Gamma_2(1 \pm \epsilon) \propto \log|\epsilon|$. The corresponding detection method for the transition would thus provide an optical

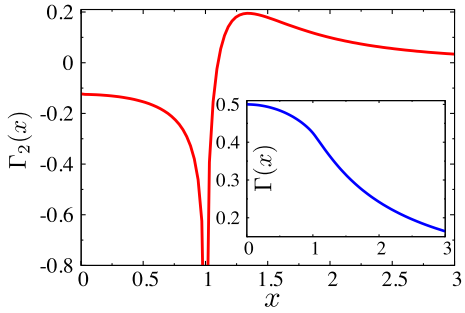

FIG. 2 (color online). The dimensionless functions $\Gamma(x)$ quantifying the microwave cavity frequency shift for an off-resonant cavity, given in Eq. (4) (inset), and $\Gamma_2(x) \equiv d^2\Gamma(x)/dx^2$ as a function of the parameter $x \equiv |\mu|/t$. There is a strong signature of the transition point $x = 1$ (i.e., $|\mu| = t$) in Γ_2, which becomes singular. The function $\Gamma(x)$ instead is continuous and monotonic, decreasing with increasing the chemical potential μ, the frequency shift being larger in the topological nontrivial phase.

alternative to the more conventional transport-based proposals such as that of Ref. [19].

In order to experimentally resolve the frequency shift, the condition $\delta\omega/\omega \gg Q^{-1}$ must be met, with Q being the quality factor of the cavity. For a typical microwave cavity, we take $\omega \sim 10^{-4}$ eV and $Q \sim 10^5$–10^6 [14], while for the tunneling matrix element t we choose $t \sim 0.1\omega$ (i.e., $t \sim 10^{-5}$ eV), corresponding to the off-resonant regime. This value of t can be achieved, for example, in coupled quantum dots gate-defined in two-dimensional semiconductor heterostructures [20]. If we assume a 1D chain of $N \sim 100$ sites, this results in a total wire length of ~ 10 μm for a unit cell size of ~ 100 nm. Note that since typical microwave cavities are millimeters long, they can easily accommodate several such artificial wires. The potential drop V_0 between the center and the ground conductors is of order $V_0 \gtrsim 1$ μeV [14], which sets itself as the upper bound for the value of α (up to a geometric capacitive factor). Using these values, we have optimistically $\alpha/\omega \sim 10^{-2}$, while for the corresponding frequency shift we obtain [using $\Gamma(\mu/t) \sim 1$] $\delta\omega/\omega \sim N(t/\omega)(\alpha/\omega)^2 \sim 10^{-3} \gg Q^{-1}$.

Resonant coupling.—In the resonant regime, it is possible to change the system topology at the single-particle level of Eq. (1) depending on the cavity state. To see this, we first simplify Hamiltonian (1) by neglecting the "counterrotating" terms that are off-resonant. Leaving the details of the derivation for the Supplemental Material [16], we show here only the final result [in the rotated particle-hole basis as described below Eq. (2)]: $\Delta H_{\rm int} = \sum_k \alpha_k^y(\tau_k^+ a + a^\dagger \tau_k^-)$, where $\alpha_k^y = \alpha\delta_k \sin\theta_k$. This closely resembles the original Dicke Hamiltonian [21]. However, note that both the single-pseudospin splittings as well as the couplings are k dependent (as opposed to the model in the previous section). For each individual k, the Hamiltonian reduces to the Jaynes-Cummings Hamiltonian, which is block diagonal, with each block being a 2×2 matrix. Each of these blocks is associated with a given value of the conserved quantity $C_k = \tau_k^z + a^\dagger a$, so that the 2×2 block acts in the subspace $\{|\uparrow_k\rangle \otimes |n\rangle, |\downarrow_k\rangle \otimes |n+1\rangle\}$. This results in an effective two-band Hamiltonian, which we can write in terms of a pseudospin $\boldsymbol{s} = (s_x, s_y, s_z)$ (Pauli matrices) as follows:

$$H_n(k) = \frac{1}{2}(\epsilon_k - \omega)s_z + \frac{\sqrt{n+1}\alpha_k^y}{2}s_x, \tag{5}$$

giving the spectrum $E_n(k) = \pm\sqrt{(\omega - \epsilon_k)^2 + (n+1)(\alpha_k^y)^2}/2$. Note that we neglected a constant shift $\Delta E_n = (n + 1/2)\omega$ of the two bands for a given $C_k = n$. For each block labeled by n, the spectrum has a band gap given by the strength of the pseudospin-photon interaction α_k^y times $\sqrt{n+1}$. This dramatically alters the initial spectrum ϵ_k, as n increases.

The single-particle picture described above is intimately related to the recent developments on the topology in periodically driven systems [12]. This connection is made concrete by considering the classical limit of a cavity prepared in a coherent state with $n \gg 1$. Neglecting the photon-number fluctuation, the single-electron spectrum then becomes $E_\pm(k) = \pm\sqrt{(\omega - \epsilon_k)^2 + \Omega_k^2}/2$, with $\Omega_k \equiv \sqrt{\langle n\rangle}\alpha_k^y$ being the classical Rabi frequency and $\langle n\rangle$ the average number of photons. The bulk topology can be correspondingly characterized by Eq. (3), with $\theta_k' \equiv \arctan[\Omega_k/(\omega - \epsilon_k)]$. We find $P' = 1$ for $t - |\mu| < \omega < t + |\mu|$, and zero otherwise. Thus the electron-photon interaction in the cavity can endow the combined system with an additional topology (here we used P' instead of P to emphasize the fact that the pseudospins in the presence of photons are of different origin than in the original Kitaev model).

The preceding results were found within a single-particle picture, which in fact loses its precise meaning in the many-body Dicke-model regime we are actually dealing with. Namely, all the pseudospins $\boldsymbol{\tau}_k$ simultaneously interact with the same cavity mode, and the exact many-body spectrum involves all of them. In order to simplify further progress, we notice that the interacting Hamiltonian admits a conserved global quantity $C = \sum_k \tau_k^z + a^\dagger a$. The simplest situation is when there are no photons in the cavity and $C = -N/2$ reaches its lowest possible value. The combined eigenstate of the system is just the product state $|\psi_{\rm tot}^0\rangle = |\Downarrow\rangle \otimes |0\rangle$ where $|\Downarrow\rangle \equiv |\downarrow \ldots \downarrow\rangle$, and the energy $E_0 = -\sum_k \epsilon_k$. For a finite number of photons in the cavity the problem becomes progressively more involved, and reasonably simple results can only be found for $n = 0$, 1, 2, as well as for $n \gg 1$ (mean field), with $n = C + N/2$.

We next wish to analyze the many-body ground state (at a fixed-n subspace) when the cavity is populated with photons. We focus only on the $n = 1$ case, as this already contains much of the relevant physics. In this case, the wave function can be expanded as

$$|\psi^1_{\rm tot}\rangle = a|\Downarrow\rangle \otimes |1\rangle + \sum_k b_k |\Downarrow;\uparrow_k\rangle \otimes |0\rangle, \quad (6)$$

where the coefficients a and b_k are found by solving the Schrödinger equation $\mathcal{H}|\psi^1_{\rm tot}\rangle = E_1|\psi^1_{\rm tot}\rangle$ [22]. The simplest case is when $\mu = 0$, so that $\epsilon_k \equiv t$, and the ground-state energy is found to be $E_1 = -(N-1)t + \omega/2 - \sqrt{N\Gamma_1 + (t-\omega/2)^2}$, with $\Gamma_1 = \sum_k (\alpha^y_k)^2/N$. (For a finite $\mu \neq 0$, the result is more complicated, albeit similar in nature.) This means the ground-state energy is lowered at resonance compared to the noninteracting situation by the amount $\propto \sqrt{N}$. If the number of pseudospins N (or the strength of coupling Γ_1) exceeds a critical value, the absolute ground state thus becomes populated with photons. For example, in the homogeneous coupling described above, $E_1 = E_0$ for $\Gamma_1 = \omega^2/N$ at resonance. Although this transition is not innately topological, it can switch the topology of the system. Thus, at the critical coupling, the system switches to a different ground state populated by photons, and the topology, which is related to the appearance of end modes, must be appropriately reexamined. To that end, however, we need to calculate the total many-body energy in a finite system, which is beyond the single-particle bulk reasoning.

Finite system.—The Majorana states are actually boundary modes, even though their existence can be inferred from the bulk spectrum. We use the discrete lattice model to numerically diagonalize the Hamiltonian in the zero- and one-photon regimes, in order to explicitly identify zero modes. We have previously noted the existence of Majorana end modes of a free chain for $\mu = 0$. That result is extended to $\mu \neq 0$, after finding an orthogonal transformation $\mathcal{M}$ such that $\tilde{H}_{\rm 1D} = \mathcal{M} H_{\rm 1D} \mathcal{M}^T = i\sum_{m=1}^N \epsilon_m \tilde{\gamma}^1_m \tilde{\gamma}^2_m$, with $\tilde{\gamma}^p_m = \sum_j s^{pr}_{mj}\gamma^r_j$ (here, $j, m = 1, \ldots, N$; $p, r = 1, 2$), $s^{pr}_{mj}(t, \mu)$ being the elements of the real orthogonal $2N \times 2N$ matrix $\mathcal{M}$ [1]. We can also write $\tilde{H}_{\rm 1D} = \sum_{m=1}^N \epsilon_m(\tilde{c}^\dagger_m \tilde{c}_m - 1/2)$, with $\tilde{c}^\dagger_m = (\tilde{\gamma}^1_m + i\tilde{\gamma}^2_m)/2$, and the eigenenergies ϵ_n define the spectrum of the chain which contain the zero modes for $|\mu| < t$.

Focusing on the topological regime, we now analyze the evolution of the many-body zero mode as the first photon is starting to populate the cavity. We assume the cavity frequency to satisfy $(t - |\mu|) < \omega < 2(t - |\mu|)$, which allows for the resonant transitions only from the Majorana states to the gapped fermionic continuum. Note that the parity of the system, $p \equiv \gamma^1_1 \ldots \gamma^2_N$, is conserved, i.e., $[p, \mathcal{H}] = 0$, which means this is a good quantum number even in the presence of the cavity. The cavity may thus affect the splitting between the parities, but not mix different parities. The interaction Hamiltonian can be written in terms of the operators $\tilde{c}^\dagger_m(\tilde{c}_m)$ instead of τ_k's which, in the rotating-wave approximation, becomes $H_{\rm int} = \sum_{m \neq m_F} A_m f(\tilde{c}_F, \tilde{c}^\dagger_F)\tilde{c}^\dagger_m a + {\rm H.c.}$, with A_m the effective coupling and $f(\tilde{c}_F, \tilde{c}^\dagger_F)$ being a linear function in $\tilde{c}_F$, $\tilde{c}^\dagger_F$. As in the pseudospin model, here too we can use the number of excitations $C \equiv \sum_{m \neq m_F} \tilde{c}^\dagger_m \tilde{c}_m + a^\dagger a$ as a conserved quantity for each parity p to find the spectrum and, as an example, we calculate the energy of the system for $C = 1$. The corresponding eigenvalues for the two parities are found from solving the eigenvalue problem similarly to Eq. (6) (see the Supplemental Material [16] for details). The splitting between the lowest-energy states of different parities in the subspace $C = 1$ is denoted by $\Delta E_{\rm maj} = |\epsilon^{\rm gs}_+ - \epsilon^{\rm gs}_-|$, while the gap to the continuum by $\Delta E_{\rm gap} = \min(\epsilon^{\rm es}_\pm) - \max(\epsilon^{\rm gs}_\pm)$, with $\epsilon^{\rm gs(es)}_\pm$ being the ground-state (excited-state) energies. Note that such a definition can be generalized for any $C \geq 1$, but not for $C = 0$.

Figure 3 shows the energy splitting between the lowest energy states, $\Delta E_{\rm maj}$, for $C = 0$ and $C = 1$, as well as the splitting (gap) between these two states and the continuum, $\Delta E_{\rm gap}$ for $C = 1$. We see that in both cases the splitting between the two states scales exponentially with the number of sites, although slower for $C = 1$. Interestingly, the energy gap $\Delta E_{\rm gap}$ saturates at a value $\propto \alpha$ for large N. Physically, the resonant interaction brings the Majorana modes into the continuum spanned by the $C = 1$ states, but as this interaction increases, precisely one state per parity is pushed below the continuum and span a well-defined two-dimensional degenerate subspace. These degenerate modes are highly entangled electron-photon states, which we call Majorana polaritons. Note that there is no Dicke-like enhancement $\sqrt{N}\alpha$ of $\Delta E_{\rm gap}$ for large N [see E_1 below Eq. (6)], since it is exactly canceled by the overlap of the Majorana states with the continuum, which scales as $1/\sqrt{N}$. Nevertheless, for large enough α, the Majorana polaritons are well defined.

The signatures of the Majorana polariton can be probed in tunneling experiments, similar to the zero energy peaks associated in the tunneling spectra with the presence of Majoranas [23–25]. For example, when the ground state of

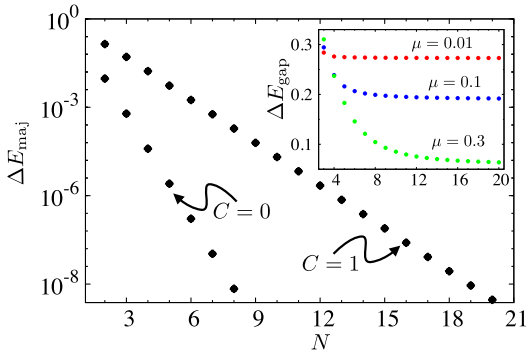

FIG. 3 (color online). Main: The energy splitting of the two lowest-energy states, $\Delta E_{\rm maj}$, for zero ($C = 0$) and one excitation ($C = 1$), as a function of the number of sites N. For these plots, we used $\mu = 0.1$, $\alpha = 0.1$, $\beta = 0$, and $\omega = 1$, all in units of t. Inset: The effective gap from the Majorana states to the continuum, $\Delta E_{\rm gap}$, for $C = 1$, as a function of N (using here $\alpha = 0.2$ to exaggerate trends).

the coupled wire-cavity system is in the $C = 0$ sector, a tunneling of an extra electron can proceed either through the Majorana mode (usual zero-bias peak), or by exciting the $C = 1$ Majorana polariton. The latter would then be manifested by a finite voltage subgap, which can be thought of as a polariton-assisted tunneling. Alternatively, the polaritonic state can be probed by the microwave transmission through the cavity, in which case the $C = 1$ subgap collective mode would appear as a resonant transmission channel. Besides that, there are other interesting issues worth careful investigation, such as the consequences of the coupling to the cavity on the braiding statistics, the boundary modes in inhomogeneous wires, as well as the fractional Josephson effect.

Summary.—To conclude, we analyzed the spectrum of a 1D Kitaev chain coupled to a microwave cavity in both off- and on-resonant regimes. We showed that the combined system exhibits highly entangled electron-photon degenerate ground states interpreted as Majorana polaritons. We expect similar phenomenology to pertain to any other physical realization of Majorana fermions that can be integrated with a microwave cavity, such as Ising spin chains [26], one-dimensional nanowires with strong spin-orbit interaction in proximity to an s-wave superconductor [7], as well as in the context of cold-atom physics [12].

This work was supported by the NSF under Grant No. DMR-0840965, the Alfred P. Sloan Foundation, and by DARPA. We gratefully acknowledge fruitful discussions with Daniel Loss.

[1] A. Y. Kitaev, Phys. Usp. **44**, 131 (2001).
[2] M. H. Freedman, A. Kitaev, M. J. Larsen, and Z. Wang, Bull. Am. Math. Soc. **40**, 31 (2003); C. Nayak, S. H. Simon, A. Stern, M. Freedman, and S. D. Sarma, Rev. Mod. Phys. **80**, 1083 (2008).
[3] M. Sato and S. Fujimoto, Phys. Rev. B **79**, 094504 (2009).
[4] L. Fu and C. L. Kane, Phys. Rev. Lett. **100**, 096407 (2008).
[5] J. Linder, Y. Tanaka, T. Yokoyama, A. Sudbø, and N. Nagaosa, Phys. Rev. Lett. **104**, 067001 (2010).
[6] M. Wimmer, A. R. Akhmerov, M. V. Medvedyeva, J. Tworzydło, and C. W. J. Beenakker, Phys. Rev. Lett. **105**, 046803 (2010).
[7] J. D. Sau, R. M. Lutchyn, S. Tewari, and S. D. Sarma, Phys. Rev. Lett. **104**, 040502 (2010); Y. Oreg, G. Refael, and F. von Oppen, Phys. Rev. Lett. **105**, 177002 (2010); R. M. Lutchyn, J. D. Sau, and S. D. Sarma, Phys. Rev. Lett. **105**, 077001 (2010); J. Alicea, Phys. Rev. B **81**, 125318 (2010); S. Gangadharaiah, B. Braunecker, P. Simon, and D. Loss, Phys. Rev. Lett. **107**, 036801 (2011).
[8] D. A. Ivanov, Phys. Rev. Lett. **86**, 268 (2001).
[9] J. Alicea, Y. Oreg, G. Refael, F. von Oppen, and M. P. A. Fisher, Nat. Phys. **7**, 412 (2011).
[10] M. Cheng, V. Galitski, and S. D. Sarma, Phys. Rev. B **84**, 104529 (2011).
[11] G. Goldstein and C. Chamon, Phys. Rev. B **84**, 205109 (2011).
[12] N. H. Lindner, G. Refael, and V. Galitski, Nat. Phys. **7**, 490 (2011); T. Kitagawa, E. Berg, M. Rudner, and E. Demler, Phys. Rev. B **82**, 235114 (2010); L. Jiang, T. Kitagawa, J. Alicea, A. R. Akhmerov, D. Pekker, G. Refael, J. I. Cirac, E. Demler, M. D. Lukin, and P. Zoller, Phys. Rev. Lett. **106**, 220402 (2011).
[13] S. Diehl, E. Rico, M. A. Baranov, and P. Zoller, Nat. Phys. **7**, 971 (2011).
[14] A. Imamoğlu, D. D. Awschalom, G. Burkard, D. P. DiVincenzo, D. Loss, M. Sherwin, and A. Small, Phys. Rev. Lett. **83**, 4204 (1999); A. Wallraff, D. I. Schuster, A. Blais, L. Frunzio, R.-S. Huang, J. Majer, S. Kumar, S. M. Girvin, and R. J. Schoelkopf, Nature (London) **431**, 162 (2004); A. Blais, R.-S. Huang, A. Wallraff, S. M. Girvin, and R. J. Schoelkopf, Phys. Rev. A **69**, 062320 (2004); M. Trif, V. N. Golovach, and D. Loss, Phys. Rev. B **77**, 045434 (2008); H. Wu, R. E. George, J. H. Wesenberg, K. Mølmer, D. I. Schuster, R. J. Schoelkopf, K. M. Itoh, A. Ardavan, J. J. L. Morton, and G. A. D. Briggs, Phys. Rev. Lett. **105**, 140503 (2010).
[15] K. Baumann, C. Guerlin, F. Brennecke, and T. Esslinger, Nature (London) **464**, 1301 (2010).
[16] See Supplemental Material at http://link.aps.org/supplemental/10.1103/PhysRevLett.109.257002 for more details on the derivations.
[17] Y. Niu, S. B. Chung, C.-H. Hsu, I. Mandal, S. Raghu, and S. Chakravarty, Phys. Rev. B **85**, 035110 (2012).
[18] F. L. Pedrocchi, S. Chesi, and D. Loss, Phys. Rev. B **83**, 115415 (2011).
[19] I. C. Fulga, F. Hassler, and A. R. Akhmerov, Phys. Rev. B **85**, 165409 (2012).
[20] R. Hanson, L. P. Kouwenhoven, J. R. Petta, S. Tarucha, and L. M. K. Vandersypen, Rev. Mod. Phys. **79**, 1217 (2007).
[21] R. H. Dicke, Phys. Rev. **93**, 99 (1954).
[22] O. Tsyplyatyev and D. Loss, Phys. Rev. B **82**, 024305 (2010).
[23] K. T. Law, P. A. Lee, and T. K. Ng, Phys. Rev. Lett. **103**, 237001 (2009).
[24] K. Flensberg, Phys. Rev. B **82**, 180516 (2010).
[25] V. Mourik, K. Zuo, S. M. Frolov, S. R. Plissard, E. P. A. M. Bakkers, and L. P. Kouwenhoven, Science **336**, 1003 (2012).
[26] Y. Tserkovnyak and D. Loss, Phys. Rev. A **84**, 032333 (2011).